

# Electron scattering of light in superconducting $Tl_2 Ba_2 CaCu_2 O_8$ single crystals

A. A. Maksimov, I. I. Tartakovskii, V. B. Timofeev, and L. A. Fal'kovskii

*Institute of Solid State Physics, Academy of Sciences of the USSR; L. D. Landau Institute of Theoretical Physics, Academy of Sciences of the USSR*

(Submitted 9 November 1989)

Zh. Eksp. Teor. Fiz. **97**, 1047–1059 (March 1990)

The electron scattering of light in superconducting  $Tl_2 Ba_2 CaCu_2 O_8$  single crystals has been studied experimentally and analytically. Temperature-dependent structural features observed in the scattering spectra measured in various crystallographic directions and for various polarizations of the light are interpreted as evidence of a pronounced anisotropy of the superconducting gap ( $2\Delta_{\min} < 50 \text{ cm}^{-1}$ ,  $2\Delta_{\max} \approx 300 \text{ cm}^{-1}$ ).

## INTRODUCTION

A central problem in the research on the new high  $T_c$  superconductors is identifying the mechanisms which are responsible for the appearance of a superconducting transition. In order to solve this problem it is important to know the superconducting gap  $\Delta$ , its  $k$ -space features, and its temperature dependence. Along with the experimental methods for determining the energy gap which are based on tunneling and far-IR spectroscopy, Raman spectroscopy can provide valuable information.

Interest in the electron scattering of light in superconductors was stimulated by the well-known paper by Abrikosov and Fal'kovskii.<sup>1</sup> According to theoretical ideas, the spectrum of electron scattering of light by a metal in its normal state should be a bell-shaped continuum and should begin at vanishingly low transition frequencies. At  $T \ll T_c$ , where  $T_c$  is the superconducting transition temperature, a dip due to the superconducting gap should appear in this spectrum. The electron-scattering spectrum of a superconductor will thus assume the shape of an asymmetric band with a sharply defined "red" boundary at an energy transfer  $\omega \approx 2\Delta$  (Ref. 1; see the diagram in Fig. 1 of the present paper). In the anisotropic case, this boundary in the electron-scattering continuum determines a minimum gap size  $\omega = 2\Delta_{\min}$  (Refs. 2 and 3).

The first experiments<sup>4-6</sup> on structural features in the electron-scattering spectra of the superconducting crystals  $Nb_3Sn$ ,  $NbSe_2$ , and  $V_3Si$ , make it possible to trace the nature of the changes in the energy gap and in the density of above-gap excitations as the temperature was varied. The use of Raman-scattering methods to study the new high  $T_c$  superconductors, specifically, to determine the value of  $\Delta$ , is extremely attractive: On the one hand, these methods are contactless methods. On the other, Raman spectroscopy has several methodological advantages over far-IR spectroscopy because of the limited transverse dimensions and inhomogeneity of the single-crystal samples.

The first attempts to detect gap features in the high  $T_c$  superconductors and to estimate their scale by electron-scattering spectroscopy were carried out on ceramic samples.<sup>7,8</sup> Later studies dealt with  $YBa_2Cu_3O_7$  (1-2-3) single crystals.<sup>9-12</sup> The difference electron-scattering spectra measured at temperatures  $T \ll T_c$  and  $T > T_c$  reveal the structural feature at  $300\text{--}350 \text{ cm}^{-1}$ , which was interpreted as the opening of a superconducting gap in this compound. Substantial

progress in the use of this method was later achieved by Klein *et al.*,<sup>13,14</sup> who studied higher-quality 1-2-3 crystals consisting of a single domain (i.e., having no twins). This research showed that low-frequency electronic excitations interact strongly with phonons of the same symmetry. An interference of discrete phonon states with the electron continuum gives the phonon lines in the light-scattering spectra the shape of antiresonances (of the Fano type). The electron-scattering spectra themselves are highly anisotropic even in the case of scattering from the basal plane. The final and most important result of these studies was the observation of an electron-scattering continuum, whose intensity was a linear function of the energy transfer at  $T \ll T_c$ , near the Rayleigh line (the unshifted line) itself (i.e., in the limit  $\omega \rightarrow 0$ ). The implication is that gap-free state exist. Because of the fundamental importance of this result, it seemed worthwhile to study electron scattering in other high  $T_c$  superconducting compounds which share a structural feature with  $YBa_2Cu_3O_7$ : $CuO_2$  planes.

In this paper we are reporting a detailed study of the electron scattering in superconducting  $Tl_2 Ba_2 CaCu_2 O_8$  crystals with a superconducting transition temperature  $T_c = 110 \text{ K}$ . A study of electron scattering in Tl-based superconductors has several features which distinguish it from

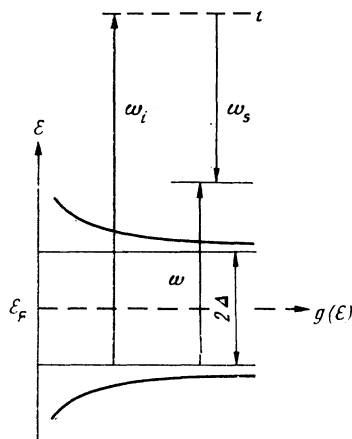


FIG. 1. Transition scheme in electron scattering of light in a superconductor.  $\omega_i$ —Frequency of the incident light;  $\omega_s$ —frequency of the scattered light;  $\omega = \omega_i - \omega_s$ —energy transfer;  $g(\epsilon)$ —density of states;  $\epsilon_F$ —Fermi energy.

corresponding studies of  $\text{YBa}_2\text{Cu}_3\text{O}_7$  and  $\text{Bi}_2\text{Sr}_2\text{CaCu}_2\text{O}_8$  crystals.<sup>15</sup> In the first place, there are no intense lines in the Raman spectra in  $\text{Tl}_2\text{Ba}_2\text{CaCu}_2\text{O}_8$  single crystals in the pertinent frequency range,  $130 < \omega < 500 \text{ cm}^{-1}$ . The reason lies in slight distortions of the cuprate planes.<sup>16</sup> Second, the shape and spectral position of the phonon components of the Raman scattering depend only weakly on the temperature. This is an exceedingly important point for detecting temperature-induced changes in the extended continuum near the superconducting gap. The more pronounced corrugation of the  $\text{CuO}_2$  planes in the  $\text{YBa}_2\text{Cu}_3\text{O}_7$  crystals gives rise to an intense Raman band of symmetry  $B_{1g}$  with a frequency  $\sim 340 \text{ cm}^{-1}$ . This band corresponds to antiphase vibrations of oxygen atoms in cuprate planes along the  $c$  axis of the crystal<sup>10</sup> and has a distinctive temperature dependence.<sup>10</sup> Finally, in the T1-2212 crystals which were studied, which have the tetragonal symmetry  $D_{4h}$ <sup>17</sup> ( $I4/mmm$ ), there is no twinning, so polarization measurements are simplified.

### EXPERIMENTAL PROCEDURE

The electron scattering was studied in T1-2212 single crystals grown from a melt of stoichiometric composition during slow cooling in an oxygen atmosphere. The samples were thin plates with a mirror-finish developed  $ab$  basal plane with dimensions  $\sim 3 \times 3 \times 0.2 \text{ mm}$ . The crystallographic structure and the lattice constants ( $a = 3.856 \text{ \AA}$ ,  $c = 29.34 \text{ \AA}$ ) were determined by x-ray diffraction. The superconducting transition temperature was  $T_c \sim 110 \text{ K}$ . Figure 2 shows data on the variation of the magnetic susceptibility  $\chi$  for one of the test samples over the temperature range  $T = 50\text{--}130 \text{ K}$ . From this figure we can easily evaluate the temperature  $T_c$  and the uniformity of the superconducting transition.

The electron-scattering spectra were studied during excitation of both the  $ab$  basal plane and the end faces of the crystal, by the line  $\lambda = 4880 \text{ \AA}$  from an  $\text{Ar}^+$  laser. The laser light was purified beforehand with the help of a diffraction grating, to eliminate the lines of the plasma discharge which lay near the lasing line. The plane of polarization of the exciting light,  $e^{(i)}$ , was rotated with the help of a  $\lambda/2$  plate. The size of the excitation region on the surface of the crystal was

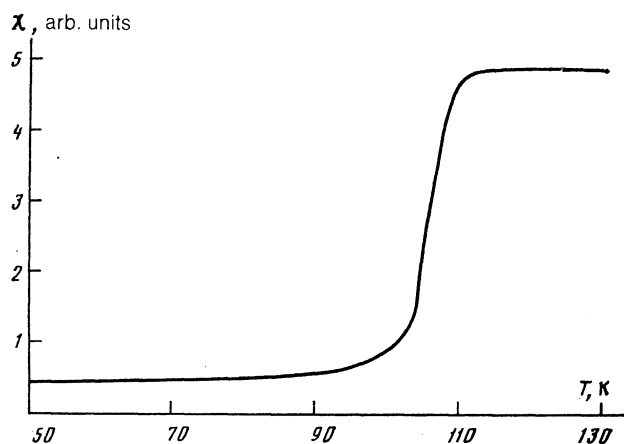


FIG. 2. Temperature dependence of the magnetic susceptibility  $\chi$  in a T1-2212 sample.

$\sim 0.05 \times 0.2 \text{ mm}^2$  in the case in which a power  $\leq 15 \text{ mW}$  was incident on the sample.

The test samples were held in He vapor in an optical helium constant-temperature chamber. This arrangement made it possible to regulate the temperature within  $\Delta T \approx \pm 0.05 \text{ K}$  over the range  $T_0 = 5\text{--}300 \text{ K}$ . At the intensities of the steady-state laser excitation which were used, the heating of the sample did not exceed  $\Delta T \leq 15 \text{ K}$  at  $T_0 = 5 \text{ K}$  according to our estimates. In view of the inhomogeneity of the samples, we measured the Raman spectra at the various temperatures at the same place on the crystal surface, with a guaranteed accuracy  $\sim 2 \mu\text{m}$ . This accuracy was monitored with the help of a microscope. The Raman spectra were measured in a backscattering geometry on a Dilor XY spectrometer equipped with a microchannel optical detector and a specially designed microscope attachment for low-temperature measurements. The laboratory  $x, y, z$  axes coincided with the crystallographic  $a, b, c$  axes, respectively. The vibrational structure in the Raman spectra was completely identical to that found in Ref. 16, where a detailed assignment of all the completely symmetric vibrational bands was made.

### EXPERIMENTAL RESULTS

Figure 3 shows Raman spectra during the excitation of the  $ab$  basal plane at two temperatures  $T_0$  in the constant-temperature chamber:  $T_0 > T_c$  and  $T_0 \ll T_c$ . We see that lowering the temperature causes a significant decrease in the intensity of the extended background  $I_s$  at frequencies  $\omega \leq 400 \text{ cm}^{-1}$ . The size of the dip at  $T_0 \approx 5 \text{ K}$  and  $\omega \approx 50$

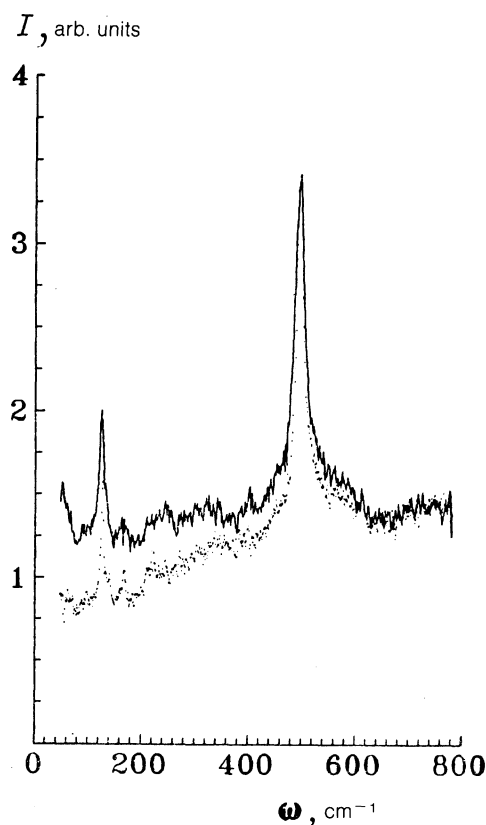


FIG. 3. Raman spectra for two temperatures  $T_0$ . Solid line—180 K; dashed line—4.5 K. The spectra were recorded in the  $z(x?)\bar{z}$  geometry.

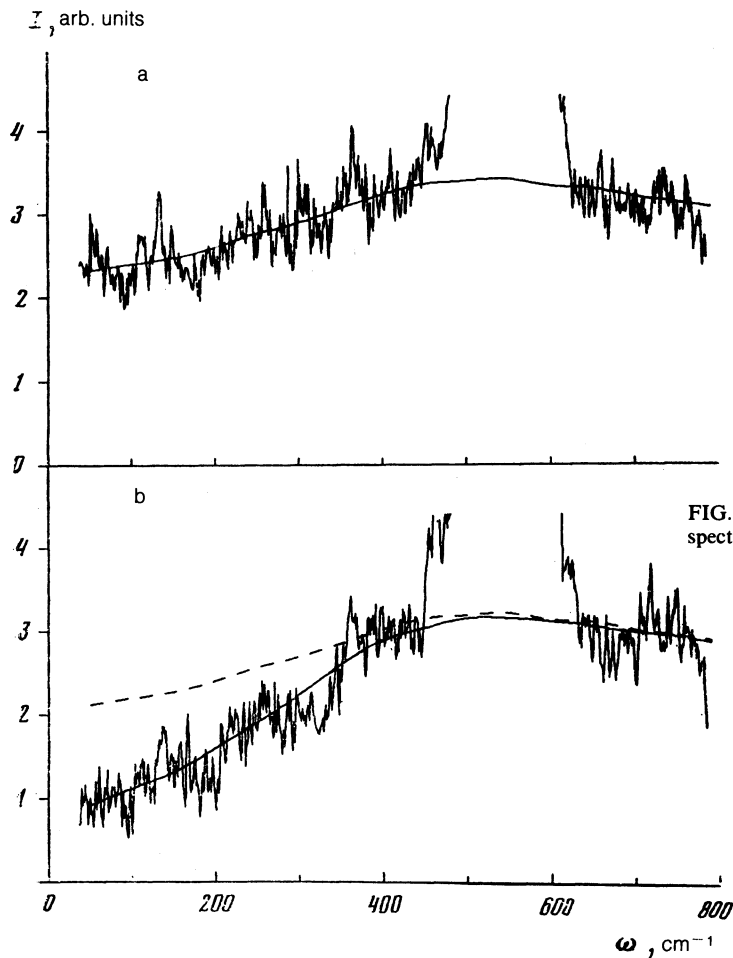


FIG. 4. Raman spectra at two temperatures  $T_0$ . a—180 K; b—4.5 K. The spectra were recorded in the  $y(zx)\bar{y}$  geometry.

$\text{cm}^{-1}$  is  $\sim 30\%$  ( $\omega = \omega_1 - \omega_s$  is the spectral shift of the electron scattering, which is reckoned from the Rayleigh line and which characterizes the energy transfer in a one-particle electron-scattering event). This value can vary over a fairly wide range, from  $\sim 10\%$  to  $\sim 80\%$ , for the various samples. Even at the lowest values of  $T_0$ , however, we did not observe  $I_s$  to decrease to zero over the range of frequencies  $\omega$  which we studied in the highest-quality samples.

The data in Fig. 4 were obtained in the geometry  $y(zx)\bar{y}$  ( $y$  and  $\bar{y} \equiv -y$  are the directions of the incident light and the scattered light, and  $z$  and  $x$  are their respective polarizations). In that geometry, the intense, completely symmetric  $A_{1g}$ -phonon components of the Raman scattering are substantially suppressed in the Raman spectra. It follows from these results that the continuous background is a broad, structureless band ranging in frequency from  $30 \text{ cm}^{-1}$  (the lower limit of the range which could be detected) to  $\sim 2000 \text{ cm}^{-1}$ . Up to  $\sim 400 \text{ cm}^{-1}$ , this background exhibits a temperature dependence.

The characteristic features of the intense, extended background observed in the Raman spectra make it possible to interpret this background as an intraband one-particle electron scattering of light by a Fermi liquid. Evidence for this interpretation comes from the following arguments.

1. The width of this band, more than  $2000 \text{ cm}^{-1}$ , is

significantly greater than the pertinent frequency range in which contributions from one- and two-photon Raman-scattering transitions could be manifested in  $\text{YBa}_2\text{Cu}_3\text{O}_{7-\delta}$  crystals.<sup>9</sup> In other words, this background is not associated with phonons. Moreover, it cannot be attributed to two-magnon scattering, since that type of scattering would be characterized by a well-expressed maximum at  $\sim 2600 \text{ cm}^{-1}$ , because of the value of the exchange integral ( $\sim 1000 \text{ cm}^{-1}$ ) for the cuprate layers.

2. Phonon lines in Raman spectra whose symmetry is that of the electron-scattering continuum have highly asymmetric shapes (Fano resonances), which are evidence of a fairly strong electron-phonon interaction.<sup>16</sup>

3. The structural features observed in the region  $\omega \leq 400 \text{ cm}^{-1}$ , which arise as the temperature is lowered ( $T_0 < T_c$ ) are naturally attributed to the presence of a superconducting gap, since the decrease in the scattering intensity in this frequency region is unambiguously correlated with the transition to the superconducting state.

Polarization measurements (Figs. 5 and 6) of electron-scattering spectra in the normal and superconducting states revealed that in all polarizations except ( $zz$ ) the decrease in the electron-scattering intensity  $I$  at  $T_0 < T_c$  sets in (with slight variations) at frequencies of about  $\omega \leq 400 \text{ cm}^{-1}$ . For the ( $zz$ ) polarization, the upper curve in Fig. 6, which corre-

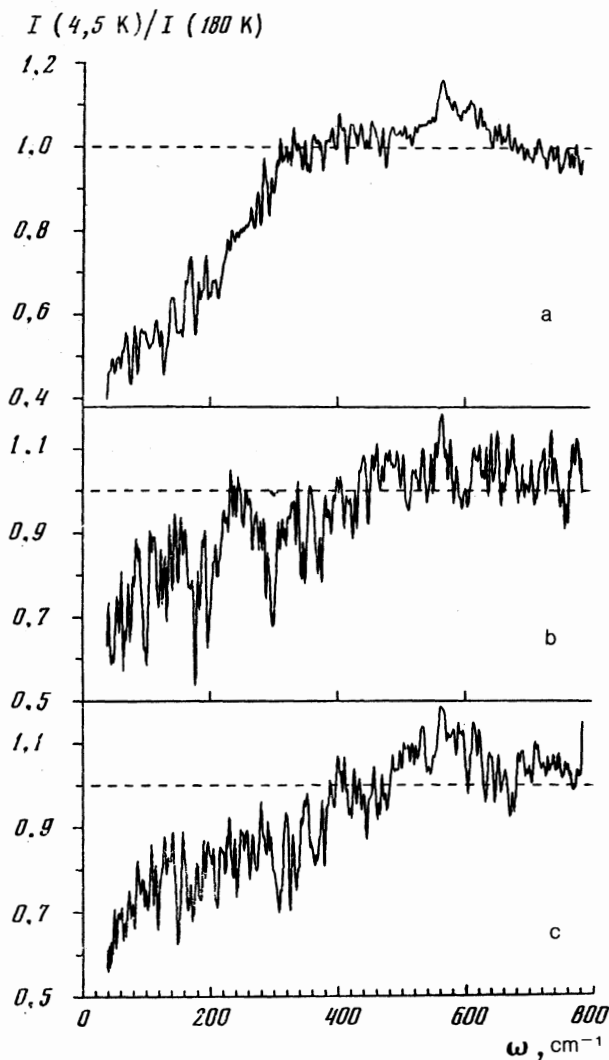


FIG. 5. Ratio of intensities  $I$  in the electron-scattering spectra at temperatures  $T \ll T_c$  and  $T > T_c$  in several configurations. a— $y(xx)\bar{y}$ ; b— $y(xz)\bar{y}$ ; c— $z(xy)\bar{z}$ .

sponds to the case in which the polarization plane of the incident light,  $e^{(i)}$ , and the scattered light,  $e^{(s)}$ , is perpendicular to the  $\text{CuO}_2$  planes, the structural feature appears in the scattering spectrum at a significantly lower frequency,  $\omega \lesssim 160 \text{ cm}^{-1}$ .

Figure 7 shows the temperature dependence of the scattering intensity,  $I$ . Specifically, this figure shows the intensity ratio  $I(T)/I(180 \text{ K})$ , found through a direct division of the experimental scattering spectra measured at several values  $T \lesssim T_c$ . We see that at  $\omega > 400 \text{ cm}^{-1}$  this ratio is essentially independent of the temperature and has a value of approximately unity (within the experimental error of  $\pm 10\%$ ). At lower frequencies  $\omega$  we see a dip, which disappears at  $T \approx T_c$ ; a further increase in the temperature causes no significant changes in the spectra. We observe a similar behavior in the  $(zz)$  polarization in Fig. 8; the implication is that this phenomenon is of the same nature. We wish to stress that the  $T$  dependence of the ratio of intensities in the vicinity of this dip in the spectra is not of an activation nature. We also note that as the temperature is raised,  $T \rightarrow T_c$ , this decrease in the size of the dip is accompanied by evidence of a tendency for the region in which the dip begins to

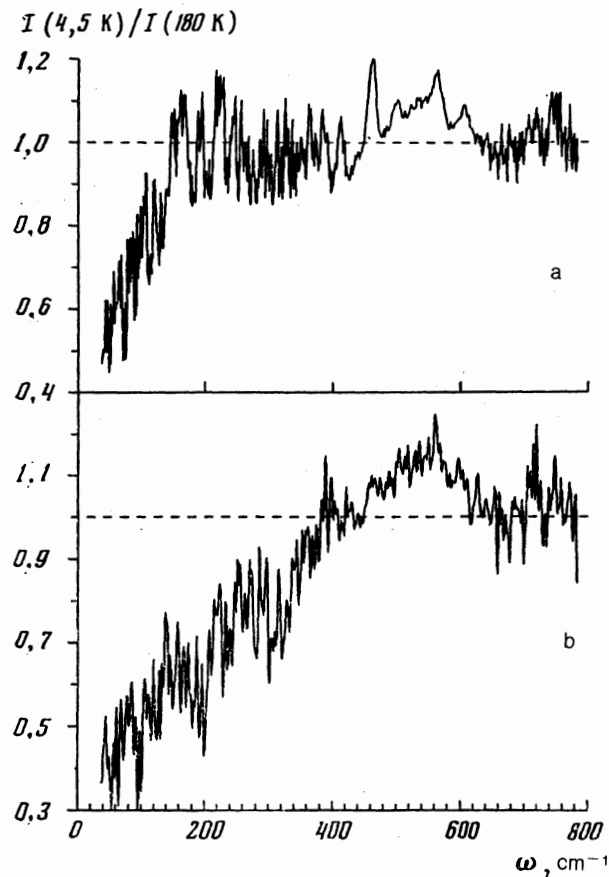


FIG. 6. Ratio of intensities  $I$  in electron-scattering spectra at temperatures  $T \ll T_c$  and  $T > T_c$ . a— $y(zz)\bar{y}$  geometry; b— $y(xz)\bar{y}$ .

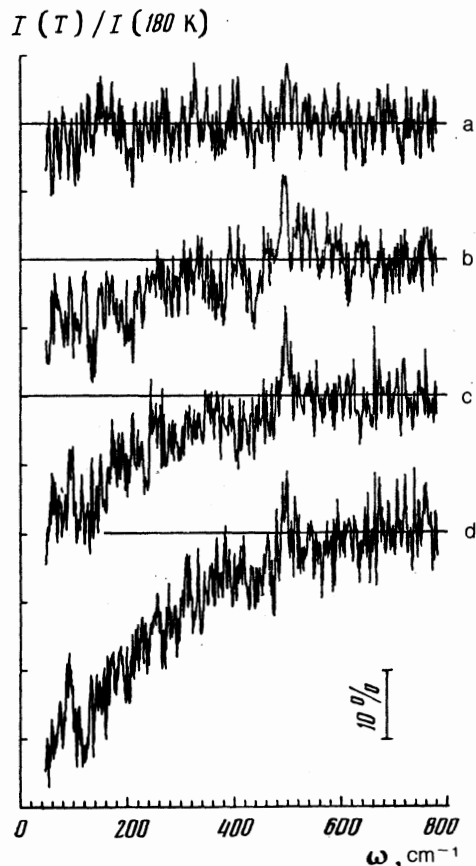


FIG. 7. Temperature dependence of the ratio of the intensities  $I$  in the electron-scattering spectra. a— $T = 110 \text{ K}$ ; b—55; c—30; d—4.5 K. The spectra were recorded in the  $z(x?)\bar{z}$  geometry.

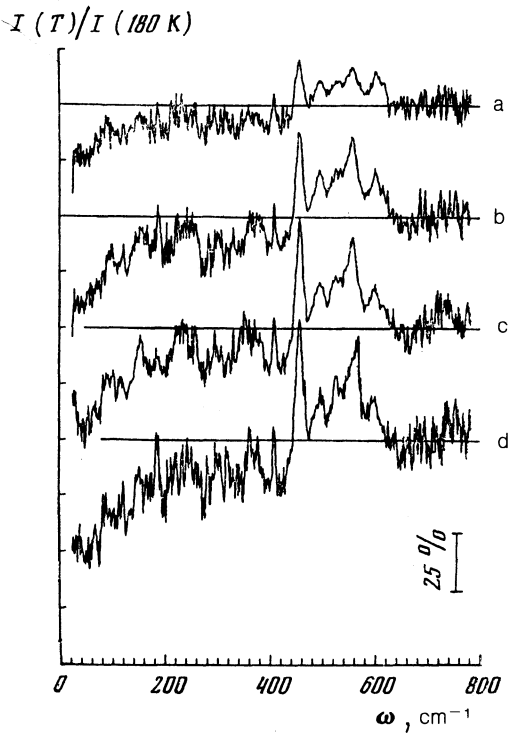


FIG. 8. Temperature dependence of the ratio of the intensities  $I$  in the electron-scattering spectra. a— $T = 110$  K; b—60; c—30; d—4.5 K. The spectra were recorded in the  $y(zz)\bar{y}$  geometry.

shift down the frequency scale. In the present study, however, we did not make a special effort to determine the temperature dependence of the spectral shift of the dip in the electron-scattering spectrum in the superconducting state.

## THEORETICAL RESULTS

Before we discuss the results, let us review the basic formulas describing the electron scattering of light in normal and superconducting metals. Despite the common assertion in the literature, the cross section for electron scattering is generally not expressed in terms of the imaginary part of the dielectric constant. That relationship holds only in an isotropic model. In the anisotropic case, a factor appears in the cross section which makes it possible to observe a scattering at values of the energy transfer below the plasma frequency, at which the dielectric constant  $\epsilon$  has no imaginary part. This factor is<sup>2,17</sup>

$$D = (e_j^{(i)} (m_{jk}^{-1} - \overline{m_{jk}^{-1}}) e_k^{(s)})^2, \quad (1)$$

where  $m_{jk}^{-1}$  is the tensor of the inverse effective mass, the superior bar means an average over the Fermi surface, and  $e^{(i)}$  and  $e^{(s)}$  are the polarization vectors of the incident and scattered light. We see that in the isotropic case we would have  $D = 0$ . Furthermore, the cross section is larger in the case in which the polarization vectors lie in the direction of small effective masses (i.e., in the  $\mathbf{ab}$  plane for layered high  $T_c$  superconductors) than in the case  $e^{(i,s)} \parallel \mathbf{c}$  axis.

We begin with the cross section in the normal phase. Here it is necessary to draw a distinction between the "clean" and "dirty" limiting cases, on the basis of whether the carrier mean free path  $l$  is large or small in comparison

with the depth to which the light penetrates into the metal,  $\delta$ . If the mean free path is large, the electron liquid consists of  $e$ - $h$  pairs in the excited state, while in the case of a short mean free path the motion of the electrons within the skin layer is a diffusion.

For clean metal ( $l \gg \delta$ ) the dependence of the cross section on the energy transfer  $\omega$  is found by taking the limit  $\Delta \rightarrow 0$  in the expressions in Ref. 1 (see also Ref. 18):

$$d\sigma = d\sigma_0 \begin{cases} (\omega\delta/v) \ln(2v/\omega\delta), & \omega \ll v/\delta, \\ 4(v/\omega\delta)^3, & \omega \gg v/\delta, \end{cases} \quad (2)$$

where

$$d\sigma_0 = \frac{4}{\pi^3} \left[ \frac{\alpha p_0}{c} \right]^2 \frac{D}{[(n+1)^2 + \kappa^2][(n-1)^2 + \kappa^2]} \frac{\delta d\omega_s}{v} d\Omega_s. \quad (4)$$

Here  $n$  and  $\kappa$  are the refractive index and attenuation coefficient at the frequency of the incident light,  $\omega_i$  ( $\epsilon^{1/2} = n + i\kappa$ ),  $p_0$  and  $v$  are the Fermi momentum and Fermi velocity,  $d\omega_s$  and  $d\Omega_s$  are the frequency interval and the solid angle of the scattered light, and  $\alpha = 1/137$  is the fine-structure constant. Unless the matter is important, we will not specifically state which momentum or velocity we have in mind for the anisotropic case.

The cross section reaches a maximum at  $\omega_{\max} \sim v/\delta$ . For  $v \sim 5 \cdot 10^7$  cm/s and  $\delta \sim 10^{-5}$  cm this quantity is, in order of magnitude,  $\omega_{\max} \sim 20$  cm $^{-1}$ .

For a dirty metal the maximum of the cross section shifts to a lower energy transfer,  $\omega_{\max} \sim vl/3\delta^2$ , and the following asymptotic expressions hold:

$$d\sigma \sim d\sigma_0 \begin{cases} \delta(\omega/vl)^{1/2}, & \omega \ll vl/3\delta^2, \\ vl/3\omega\delta^2, & vl/3\delta^2 \ll \omega \ll v/l, \\ v^3/\omega^3 l\delta^2, & \omega \gg v/l. \end{cases} \quad (5)$$

$$d\sigma \sim d\sigma_0 \begin{cases} vl/3\omega\delta^2, & vl/3\delta^2 \ll \omega \ll v/l, \\ v^3/\omega^3 l\delta^2, & \omega \gg v/l. \end{cases} \quad (6)$$

$$d\sigma \sim d\sigma_0 \begin{cases} v^3/\omega^3 l\delta^2, & \omega \gg v/l. \end{cases} \quad (7)$$

The decrease in (6), slower than that in (3), occurs over a fairly wide frequency interval.

We turn now to the electron scattering in a superconductor. We restrict this discussion to the clean case. We need to draw a distinction between two qualitatively different situations. For the conventional superconductors the so-called limit of a large vector transfer,  $v/\delta \gg \Delta$ , is valid (the vector transfer is on the order of  $1/\delta$ ), and the expressions of Refs. 1 and 2 can be used. As  $\delta$  here we must take the depth to which the light penetrates into the metal at the frequency  $\omega_i \approx \omega_s$ , which is large in comparison with  $\Delta$  in the optical range. The superconductivity naturally has no effect on the value of  $\delta$  here.

According to Refs. 1 and 2, there is a threshold  $\omega_{\text{thr}} = 2\Delta_{\min}$  in the spectrum, which is set by the minimum value of the gap on the belt belonging to the Fermi surface, where the electron velocity runs parallel to the surface of the sample. We wish to stress that the cross section does not change discontinuously near the threshold. It vanishes continuously both in an isotropic superconductor (in which case a chain of diagrams which is infinite in the electron interaction must be taken into account) and in an anisotropic superconductor, in which case the number of final elec-

tron states decreases as  $\omega$  approaches the threshold from above.

At this point we are interested in a superconductor for which the limit of a small vector transfer,  $v/\delta \ll \Delta$ , holds. If the minimum size of the gap on the Fermi surface,  $\Delta_{\min}$ , is nonzero, then there is a threshold  $\omega_{\text{thr}} = 2\Delta_{\min}$  in the scattering spectrum again in this case at absolute zero.<sup>3</sup> The threshold in this case depends on neither the direction of the normal to the surface of the sample nor the polarization vectors.

The frequency dependence of the cross section is determined to a large extent by the angular dependence of the energy gap. Let us consider three different cases.

1. The anisotropy of the gap is slight. There then exists a threshold energy transfer  $\omega_{\text{thr}} = 2\Delta$  below which no scattering occurs. Above the threshold we can use the following asymptotic expressions:

$$d\sigma = d\sigma_0 \begin{cases} \frac{4}{\pi} \frac{\xi^3}{\delta^3} \frac{\ln(\delta/\xi)}{\ln(\xi_1/\delta) \ln(\xi_1/\xi)}, & (\omega^2 - 4\Delta^2)^{1/2} \ll v/\delta, & (8) \\ \frac{4}{\pi} \frac{\xi^3}{\delta^3}, & v/\delta \ll (\omega^2 - 4\Delta^2)^{1/2} \ll \Delta, & (9) \\ 4 \left( \frac{v}{\omega\delta} \right)^3, & \omega \gg 2\Delta, & (10) \end{cases}$$

where  $\xi = v/\Delta$ , and  $\xi_1 = v/(\omega^2 - 4\Delta^2)^{1/2}$ . We wish to stress that expressions (8)–(10) describe a broad maximum. Its width is on the order of  $\Delta$ , i.e., the same as the distance to the unshifted line.

2. The superconductor has a substantially anisotropic gap, which vanishes nowhere on the Fermi surface. In this case the threshold is set by the smallest value of the gap on the Fermi surface. The threshold does not depend on the polarization of the incident or scattered light. Near the threshold the cross section behaves in different ways, depending on whether the minimum of  $\Delta$  is reached at a point or on a line on the Fermi surface (the latter case is possible, in particular, for quasi-two-dimensional superconductors):

$$d\sigma \sim d\sigma_0 \begin{cases} [(\omega - 2\Delta_{\min})/\Delta_{\min}]^{1/2}, & (\text{minimum at point}), \\ \ln \left[ \frac{\Delta_{\min}}{\omega - 2\Delta_{\min}} \right]^{-2}, & (\text{minimum on line}). \end{cases} \quad (11)$$

With distance from the threshold the cross section decreases when the energy transfer  $\omega$  increases by an amount on the order of the maximum gap size,  $2\Delta_{\max}$  (the maximum value on the Fermi surface).

3. The gap vanishes at certain points or on certain lines which belong to the Fermi surface. The cross section has no threshold. It does have a maximum at an energy transfer on the order of the maximum gap size. With decreasing frequency, the cross section decreases linearly if gap vanishes on a line, or it decreases quadratically when the gap vanishes at isolated points.

## DISCUSSION

On the basis of our experimental data we can estimate  $I_s$ , the intensity of the light in the extended continuum which is scattered into an angle  $d\Omega_s = 1$  in the spectral interval  $d\omega_s \approx 20 \text{ cm}^{-1}$ , divided by the intensity of the incident light:  $I_s/I_i \approx 0.3 \cdot 10^{-12}$ . At a distance on the order of  $\Delta$  from the threshold, the coefficient of  $d\sigma_0$  in expression (11) reaches a value on the order of unity, and a theoretical esti-

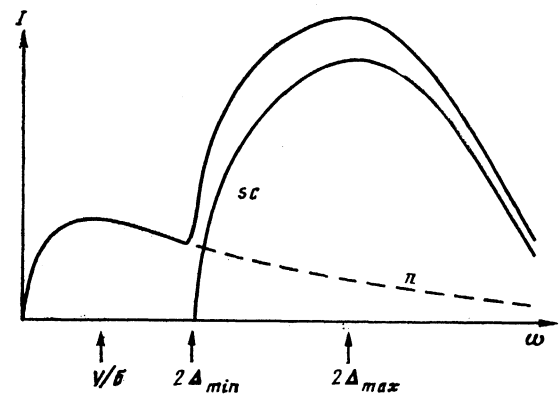


FIG. 9. Shaping of the resultant electron-scattering spectrum during the superposition of the electron-scattering spectra of the normal phase ( $n$ ) and of the superconducting phase ( $sc$ ).

mate from (4) yields  $I_s/I_i \approx 2 \cdot 10^{-12}$  if we take  $n = 1.2$  and  $\kappa = 1$  from the optical measurements, assume  $v = 0.5 \cdot 10^8 \text{ cm/s}$ , and note that we have  $d\omega_s \delta/v \approx 1$  for  $d\omega_s = 20 \text{ cm}^{-1}$ . Since the theoretical estimate is extremely sensitive to  $\kappa$  and  $v$ , we judge the agreement with experiment satisfactory.

An important feature is the behavior of the scattering cross section in the limit  $\omega \rightarrow 0$ . According to our observations, the cross section does not vanish in this case, while the theory of electron scattering predicts that it should decrease to zero, regardless of whether the metal is in a normal or superconducting state. For a normal metal, however, the decrease cannot begin at an energy transfer  $\omega > v/\delta$ . For a dirty normal metal, the decrease begins at even smaller values of  $\omega$ . The data available support only the approximate estimate  $v/\delta \approx 20 \text{ cm}^{-1}$ , which shows that our observations fall in a region in which the decrease in the cross section toward smaller values of  $\omega$  should not yet occur. Taking that circumstance into account, and also noting that the size of the dip in the cross section at low temperatures for  $\omega \approx 50 \text{ cm}^{-1}$  varies from 10% to 80% for the various samples, we conclude that our samples contained foreign, nonsuperconducting phases (the content of the foreign phases could locally have a significant effect on the scattering of light, despite the fact that the x-ray diffraction analysis guarantees the content of the T1-2212 phase by volume within  $\sim 2\%$ ). The situation is shown schematically in Fig. 9, which explains the behavior of the electron scattering for an energy transfer  $\omega > v/\delta$  in a normal metal and in a superconductor with a normal-phase impurity.

For certain samples, nevertheless, the cross section decreased nearly to zero at a small transfer. In principle, this effect might be attributed to the existence of excitations below the gap. If we are talking about electronic excitations, however, their number decreases in proportion to  $\exp(-\Delta/T)$  with the temperature, and this factor becomes exceedingly small at low temperatures. We are left with the suggestion that the superconducting gap vanishes somewhere on the Fermi surface, or that, in any case, its minimum value does not exceed  $2\Delta_{\min} < 50 \text{ cm}^{-1} \approx 0.6k_b T_c$ , as can be seen from our data. In order to explain the linear dependence of the cross section at a small energy transfer, we should assume that the gap disappears (or assumes a sufficiently small value) along lines lying on the Fermi surface.

Let us examine the possibility of determining the maximum size of the gap from the electron-scattering data. It can be seen from Fig. 9 that in a superconductor the scattering forms a broad continuum with a maximum at about  $\omega \approx \Delta_{\max}$ . The position of this maximum, in contrast with the threshold  $2\Delta_{\min}$ , depends on integral characteristics of the electron spectrum, e.g., the factor  $D$  in (1), which is in turn determined by the directions of the polarization vectors. One thus cannot work from the position of the maximum (or from the value of the frequency at which the scattering in the superconductor differs from that in a normal metal; cf. Figs. 5 and 6) to reach the conclusion that the gap depends on the polarization direction, although this is sometimes done. The maximum value of the gap can be estimated. We see from Figs. 5 and 6, that such an estimate yields  $2\Delta_{\max} \approx 300 \text{ cm}^{-1} \approx 4k_b T_c$ .

We are deeply indebted to A. A. Abrikosov, D. E. Khmel'nitskiĭ, and G. M. Éliashberg for useful discussions and comments.

<sup>1</sup> A. A. Abrikosov and L. A. Fal'kovskii, Zh. Eksp. Teor. Fiz. **40**, 263 (1961) [Sov. Phys. JETP].

<sup>2</sup> A. A. Abrikosov and V. M. Genkin, Zh. Eksp. Teor. Fiz. **65**, 842 (1973) [Sov. Phys. JETP **38**, 417 (1974)].

<sup>3</sup> A. A. Abrikosov and L. A. Falkovsky, Physica C **156**, 1 (1988).

- <sup>4</sup> R. Sooryakumar and M. V. Klein, Phys. Rev. Lett. **45**, 660 (1980); Phys. Rev. B **23**, 3213 (1981).
- <sup>5</sup> S. B. Dierker, M. V. Klein, G. W. Webb, and Z. Fisk, Phys. Rev. Lett. **50**, 853 (1983).
- <sup>6</sup> R. Hackl, R. Kaiser, and S. Schicktanz, J. Phys. C **16**, 1729 (1983).
- <sup>7</sup> A. V. Bazhenov, A. V. Gorbunov, N. V. Klassen, *et al.*, Pis'ma Zh. Eksp. Teor. Fiz. **46**, Supplement, 35 (1987) [JETP Lett. **46**, Supplement, S29 (1987)].
- <sup>8</sup> K. B. Lyons, S. H. Lion, M. Hong, *et al.*, Phys. Rev. **36**, 5592 (1987).
- <sup>9</sup> S. L. Cooper, M. V. Klein, B. J. Pazol, *et al.*, Phys. Rev. B **37**, 5920 (1988).
- <sup>10</sup> C. Tomsen and M. Cardona, in *Physical Properties of High Temperature Superconductors 1* (ed. D. M. Ginsberg), World Scientific, Singapore, 1989, Ch. 8.
- <sup>11</sup> Yu. A. Ossipyan, V. B. Timofeev, I. F. Shegolev, *et al.*, Physica C **153-155**, 1133 (1988).
- <sup>12</sup> R. Hackl, W. Glessr, P. Meller, *et al.*, Phys. Rev. B **38**, 7133 (1988).
- <sup>13</sup> S. L. Cooper, F. Slakey, M. V. Klein, *et al.*, J. Opt. Soc. Am. **6**, 436 (1989).
- <sup>14</sup> S. L. Cooper, F. Slakey, M. V. Klein, *et al.*, Phys. Rev. B **38**, 11934 (1988).
- <sup>15</sup> D. Kirillov, I. Bozovic, B. H. Geballe, *et al.*, Phys. Rev. B **38**, 11955 (1988).
- <sup>16</sup> L. V. Gasparov, V. D. Kulakovskii, O. V. Misochko, *et al.*, Physica C **160**, 147 (1989).
- <sup>17</sup> L. A. Fal'kovskii, Zh. Eksp. Teor. Fiz. **95**, 1145 (1989) [Sov. Phys. JETP **68**, 661 (1989)].
- <sup>18</sup> I. P. Ipatova, M. I. Kaganov, and A. P. Subashiev, Zh. Eksp. Teor. Fiz. **84**, 1830 (1983) [Sov. Phys. JETP **57**, 1066 (1983)].

Translated by Dave Parsons